

Silver cation-mediated dual-emissive Au–Ag bimetallic nanoclusters for pH ratiometric sensing

Bo Peng,^a Liu-Xi Zheng,^a Pan-Yue Wang,^a Jia-Feng Zhou,^a Meng Ding,^a Hao-Di Sun,^a Bing-Qian Shan*^a, Kun Zhang*^{a,b,c}

^aShanghai Key Laboratory of Green Chemistry and Chemical Processes, College of Chemistry and Molecular Engineering, East China Normal University, Shanghai 200062, China;

^bLaboratoire de chimie, Ecole Normale Supérieure de Lyon, Institut de Chimie de Lyon, Université de Lyon, 46 Allée d'Italie, 69364 Lyon cedex 07, France;

^cShandong Provincial Key Laboratory of Chemical Energy Storage and Novel Cell Technology, School of Chemistry and Chemical Engineering, Liaocheng University, Liaocheng, 252059, Shandong, P. R. China

* Correspondence: bqshan_ecnu@163.com and kzhang@chem.ecnu.edu.cn (K.Z.)

Abstract: Metal nanoclusters (NCs) with intrinsic dual-emission are not only significant for fundamental research but also for accurate ratiometric sensing and imaging. Using 1-dodecanethiol (DT) as protected-cum-reduced ligand, the core-shell structured Au-Ag bimetallic NCs with well-resolved dual-emission bands centered at 440 nm and at 630 nm were successfully synthesized by a facile one-pot approach. A combined characterizations of X-ray photoelectron spectroscopy (XPS), transmission electron microscope (TEM) and optical spectrum revealed that the Au-Ag bimetallic NCs had a core-shell structure with a metallic Au(0) core coated by a shell of Au(I)- and Ag(I)-thiolate motifs. Very interestingly, the dual-emissive Au-Ag NCs exhibited unique ratiometric pH-dependent emissions, which could be used as an ideal pH ratiometric nanosensors. Most importantly, our observed Ag⁺ mediated pH-dependent dual-emissive behavior suggests that the metal NCs core is not a real emitter center, while structural water molecules (SWs) confined at the nanoscale interface of metal core are true luminous centers, which answers that the optical properties of metal NCs are very sensitive to the delicate change of surrounding microenvironment of metal NCs, including the dosing of Ag⁺, pH and packing mode of surface ligands. Our discovery not only opens up new possibilities for the design of ultra-small ratiometric pH nanoindicators, but also provides new insights on the origin of photoluminescent (PL) emission of metal NCs.

Introduction

Quantum sized metal nanoclusters, that bridging the gap between organometallics and nanocrystals, exhibit dramatically unique electronic and optical properties, such as molecule-like energy gaps^[1-8], intense photoluminescence^[9-13] and catalytic properties^[14-20]. Luminescent thiolated-protected Au and Ag NCs in particular have attracted tremendous interest due to their wide applications in bio-imaging, bio-medicine, sensing and catalysis, etc^[21-29]. Various strategies, such as heteroatom doping^[30], aggregation-induced-emission (AIE)^[12], assembly induced emission enhancement^[31], *etc.* have been developed to prepare highly luminescent Au and Ag NCs. Since the crystal structure of ligand-protected Au NCs, which usually comprised by metallic core and peripheral gold(I)-thiolate staple motifs, have been revealed at atomic resolution^[32], heteroatom substitution of specific native sites could give an in-depth sight to understand the structure/composition-correlated properties and provided an efficient way to diversify and tailor

the physicochemical properties of metal NCs^[33, 34]. Several strategies have been developed to the synthesis of bimetallic Ag-Au NCs, such as one-pot co-reduction method^[35-37] (spontaneous reduction of as-mixed Ag and Au precursors through balancing the redox potentials of metal pairs by thiol ligand^[38, 39]), classical galvanic replacement reaction approach^[40] (involves the spontaneous reduction of a noble-metal cationic by a less noble metal in solution driven by the difference in redox potentials), abnormal anti-galvanic replacement reaction approach^[41, 42] (inverse process for galvanic replacement reaction recently observed for the synthesis of thiolate-protected Ag-Au NCs) and addition reaction^[43-45] (a hydride-mediated controlled growth process), etc. And intriguingly, as-formed heteroatom doped metal NCs generally exhibited dramatically enhancement of luminescent and catalytic performance^[30, 46-52], which are expected to have synergistic effects in their physicochemical properties compared with their mono-metallic analogues^[53]. Nevertheless, the origin of PL or the nature of emitter of heteroatom doped metal NCs remain unclear and even controversial, which limits the rational design of metal nanoclusters with improved and tailored optical and catalytic properties.

Luminescent metal NCs with dual-wavelength emission have been exploited as ratiometric nanoprobes for sensing and imaging^[54], rather than absolute intensity-dependent signal readout of single-emissive metal NCs, ratiometric measurements provide built-in self-calibration for signal correction, enabling more sensitive and reliable detection, which imposed the metal NCs possess two target-responsive reversible signal changes or one of the signal is target-insensitive as reference^[55, 56]. However, in most cases, well-resolved dual-wavelength emission of metal NCs was rarely observed simultaneously. Herein, we demonstrated that, using 1-dodecanethiol (DT) as a protected ligand, Au-Ag bimetallic NCs can be readily synthesized by a facile one-pot approach, exhibiting an interesting silver cation-mediated dual-emission behavior at 440 nm and 630 nm. Very interestingly, the dual-emissive Au-Ag bimetallic NCs display a unique reversible environment-pH-responsive emission behavior, which makes them ideal as potential pH ratiometric sensors: at acid conditions, the long-wavelength emission at 630 nm is dominated, while at basic conditions, the short-wavelength emission at 440 nm is prevailed. The combined characterizations of absorption, excitation and emission spectrum evidenced that the dual-emissions come from the same luminous center, *i.e.*, structural water molecules (SWs) dynamically confined on the metal NCs core, but with varied binding strength with surface Au(I)- and Ag(I)-thiolate motif, corresponding to the emission at 630 nm and 440 nm, respectively. The assignment of SWs as emitters is consistent our previously reported results,^[57, 58] which also answers that the efficiency of dual-emissions is very sensitive to the delicate change of surrounding microenvironment of metal NCs, including the dosing of Ag⁺, pH and packing mode of surface ligands since the surface states formed by space overlapping of p orbitals of O atoms in the SWs {H₂O·OH} as dynamic feature with π bonding nature.

Results and discussion

The synthesis protocol of Au-Ag@DT NCs using DT as protected-cum-reduced ligand was modified from the previously reported method^[49]. Ag(I)-complexes was firstly formed by mixing DT alcoholic solution and AgNO₃ under vigorous stirring for 10 min. HAuCl₄ solution was then added into the mixed solution and the mixtures were further stirred 12 h and incubated overnight at room temperature, the obtained samples denoted as Ag_xAu@DT NCs, which the x represented the feeding ratio of Ag to Au (synthesis details in the ESI). The incorporation of silver and gold to form Ag_xAu@DT NCs was evidenced through the thermogravimetric analysis

(TGA) and inductively coupled plasma (ICP) atomic emission spectroscopy (Fig. S1 and Tab. S1), with increasing the feeding ratio of Ag-Au from 0.25, 0.5, 1, 2 and 4, the actual ratio of Ag to Au in the obtained NCs analyzed through ICP was determined as 0.11, 0.23, 0.47, 1.02 and 1.25, respectively, and the ligand weight loss (Fig. S1) was also gradually increased from 47.57% to 61.80%, stoichiometric formula of obtained $\text{Ag}_x\text{Au}@DT$ NCs can be estimated as $\text{Ag}_0\text{Au}_1\text{DT}_{0.9}$, $\text{Ag}_{0.1}\text{Au}_1\text{DT}_{1.2}$, $\text{Ag}_{0.2}\text{Au}_1\text{DT}_{1.4}$, $\text{Ag}_{0.5}\text{Au}_1\text{DT}_{1.5}$, $\text{Ag}_1\text{Au}_1\text{DT}_{2.2}$ and $\text{Ag}_{1.3}\text{Au}_1\text{DT}_{2.7}$ respectively (Tab. S1), As show in Fig. 1a and b, with increasing the feeding ratio of Ag to Au, a new narrow blue emission band centered at 440 nm of $\text{Ag}_x\text{Au}@DT$ NCs was generated and then boosted, and the inherent red emission band centered at 630 nm of Au NCs was concomitantly declined, showing a relation of ‘as one falls, another rises’ (Fig. 1b). In a range of Ag/Au molar ratio from 0.25 to 2.0, because of the color mixing of dual-emissions, the as-synthesized Au-Ag bimetallic NCs exhibited the bright purple photoluminescence under UV irradiation of both 260 nm and 365 nm (Fig. 1a). However, if further Ag^+ doping with Ag/Au molar ratio of 4.0, the single emission at 630 nm of monometallic Au NCs was almost completely disappeared, only a sharp and strong emission band center at 440 nm was observed for $\text{Ag}_4\text{Au}@DT$ NCs (Fig. 1b). Time-resolved PL spectroscopy showed that the radiation decay of blue and red emission channels had distinguished lifetimes of 5.4 nanoseconds (ns) and 2.0 microseconds (μs), respectively (Fig. 1d). It is importantly noted that, if according to conventional quantum size confinement mechanics of metal NCs, the inherent long-wavelength emission at 630 nm from Au core could not be disappeared since the Au NCs core remains intact with the increase of Ag^+ loading (Fig. S2), suggesting the irrationality of Au NCs as emitters.

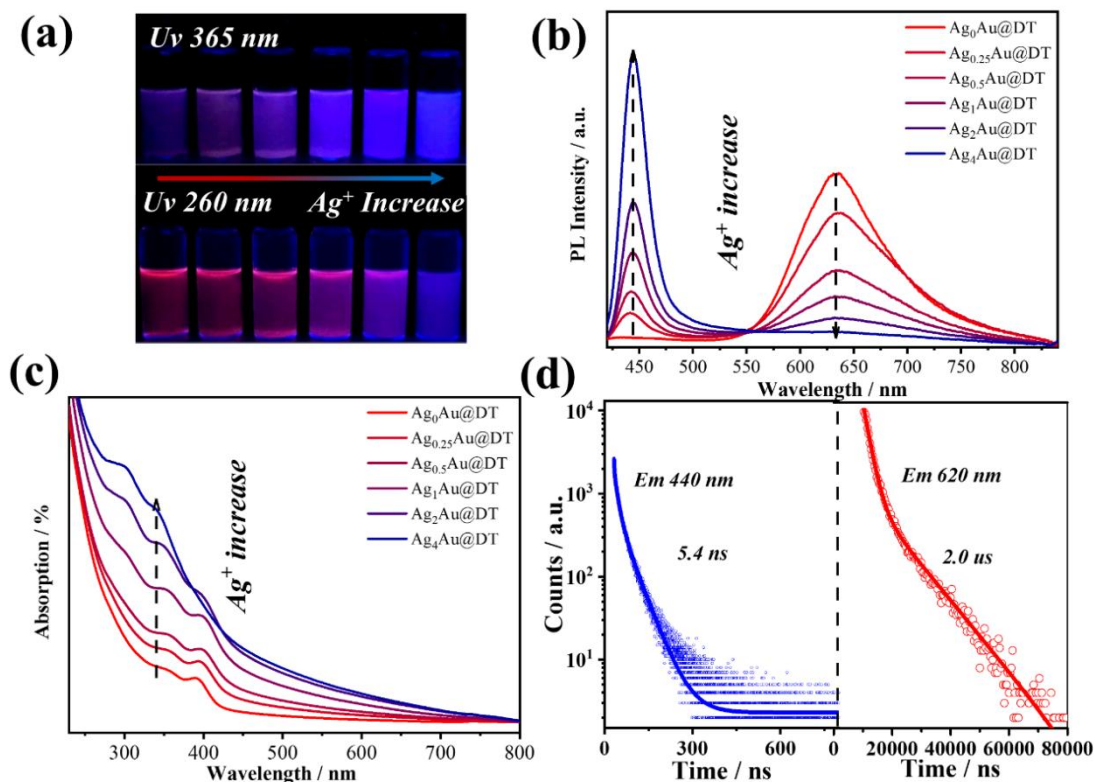


Figure 1. (a) Luminescent photographs of $\text{Ag}_x\text{Au}@DT$ NCs under UV 365 nm (top) and 260 nm (bottom) irradiations. Photoluminescence emission spectra (b) and absorption spectra (c) of $\text{Ag}_x\text{Au}@DT$ NCs. (d) Time-resolved luminescence decay profiles of $\text{Ag}_1\text{Au}@DT$ NCs measured at 440 nm (left panel) and 630 nm (right panel), respectively.

The UV-visible absorption spectrum of $\text{Au}_x\text{Ag}@\text{DT}$ was collected in Fig 1c. Without the doping of silver, the Au NCs showed three remarkable absorption peaks located at 285 nm, 350 nm and 390 nm, respectively, which has been previously assigned to Au 6sp intraband and interband transitions of Au NCs with 10~12 atoms^[3]. The absence of localized surface plasmon resonance bands at 420 nm in the absorption spectrum implies that the particle size of Au-Ag bimetal is in the range of metal nanoclusters, consistent with the results of TEM (Fig. 2a and Fig. S2). Interestingly, with the increasing feeding ratio of Ag to Au, the intensity of absorption bands at 350 and 390 nm is not changed, while the absorption at 285 nm is gradually intensified. Thus we assigned the absorptions at 350 nm and 390 nm to the Au 6sp intraband and interband transitions of Au NCs without the size change of Au NCs core, while the intensified adsorption at 285 nm is attributed to the ligand (thiol) to metal (Au^+ or Ag^+) charge transfer (LMCT), consistent with an ascending trend of molar ratio of DT/Ag in Au-Ag bimetal NCs (Fig. S1 and Tab. S2) with more dosing of Ag^+ . Thus, we supposed that the Au-Ag bimetal NCs had a core-shell structure with Au NCs core coated by Au- and / or Ag-thiolate motifs. But, we cannot confirm the valence charge states of metals.

High-resolution transmission electron microscopy (HRTEM) and X-ray photoelectron spectra (XPS) characterizations supported this hypothesis. HRTEM images (Fig. 2a) corroborated the size of as-formed $\text{Ag}_1\text{Au}@\text{DT}$ NCs of *ca.* 1.7 nm and no variation with the doping of silver (Fig. S2). The measured inter-planar distance from fringes in HRTEM images (0.24 nm, Fig. 2a insert) corresponds to the (111) plane of the cubic phase structure of Au (JCPDS ID 04-0784). The XPS was used to analyze the valence charge state of metal and composition of Au-Ag bimetal NCs (Fig. 2 b-d). As shown in the Ag 3d spectra (Fig. 2b), the oxidation state of silver was all Ag(I) components with binding energy of 367.8 eV, suggesting the single Ag(I)-thiolate species in the $\text{Ag}_1\text{Au}@\text{DT}$ NCs^[46], and the Au 4f spectra (Fig 2c) were deconvoluted into Au(I) and Au(0) components with binding energies of 84.0 and 85.2 eV, respectively, and the content of Au(I) determined as such only account small fraction (~5%) of all Au atoms in the $\text{Ag}_1\text{Au}@\text{DT}$ NCs. As reference to conventional Au-thiolate NCs^[12, 59], this value is significantly lower and is the consequence of the substitution of Au(I)-thiolate staple motifs by incoming Ag(I)-thiolate.

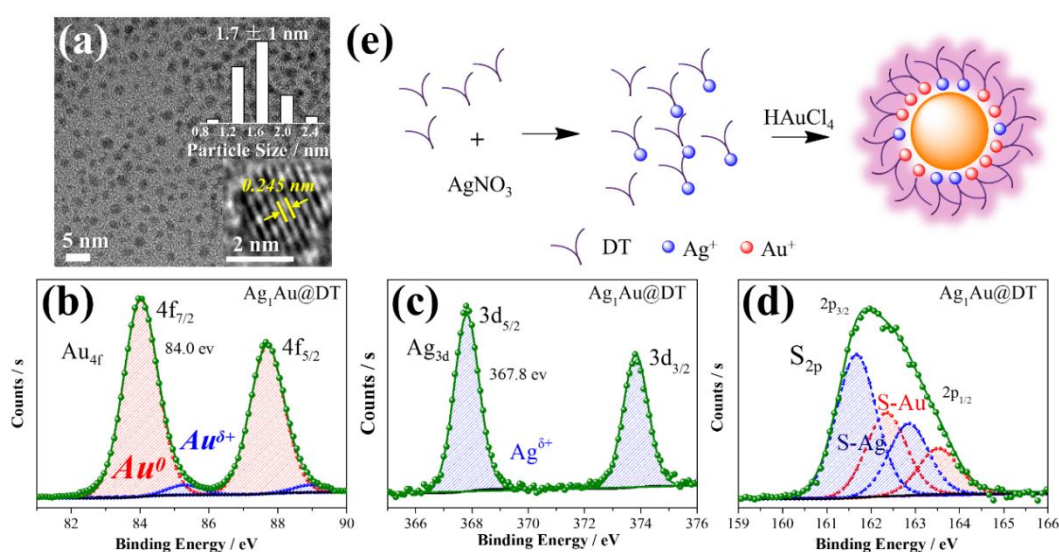


Figure 2. (a) Scheme for the synthesis process of $\text{Ag}_1\text{Au}@\text{DT}$ NCs. TEM (b) and XPS spectrum of Au 4f (c), Ag 3d (d) and S 2p (e) for $\text{Ag}_1\text{Au}@\text{DT}$ NCs.

More prominent results were demonstrated by the deconvolution of S 2p spectra (Fig. 2d), two distinct components with binding energies of 161.7 eV and 162.3 eV were assigned to the Au(I)-thiolate and Ag(I)-thiolate, respectively. The content of the later one was increased with the increasing feed ratio of Ag to Au (Fig. S3 and Tab. S2), which is consistent to the ICP and TGA results. The detailed fitting result is summarized in Table S2. Therefore, a scheme was illustrated for the formation process of core-shell structured $\text{Ag}_1\text{Au@DT}$ NCs. Initially, Ag(I)-thiolate complexes were formed after the mix of DT and AgNO_3 , due to the lower redox potential of Ag^+/Ag (0.8 eV) than $\text{AuCl}_4^-/\text{Au}$ (1.0 eV) and the fast etching kinetics of Ag(I)-thiolate^[60], Ag(I)-thiolate was not reduced in this synthetic protocols, the subsequently added HAuCl_4 was reduced and protected by DT to form the metallic Au(0) core which stapled Ag(I)-thiolate and Au(I)-thiolate motifs together. Obviously, according to well-accepted quantum size confinement effect of metal NCs with zero charge state, the surface thiolate- Ag^+ motif could not be the emitter center of short-wavelength at 440 nm. Overall, our results of dual-emission of Au-Ag bimetal NCs mediated by Ag^+ doping cannot support the quantum size confinement mechanics for the elucidation of origin of PL of metal NCs.

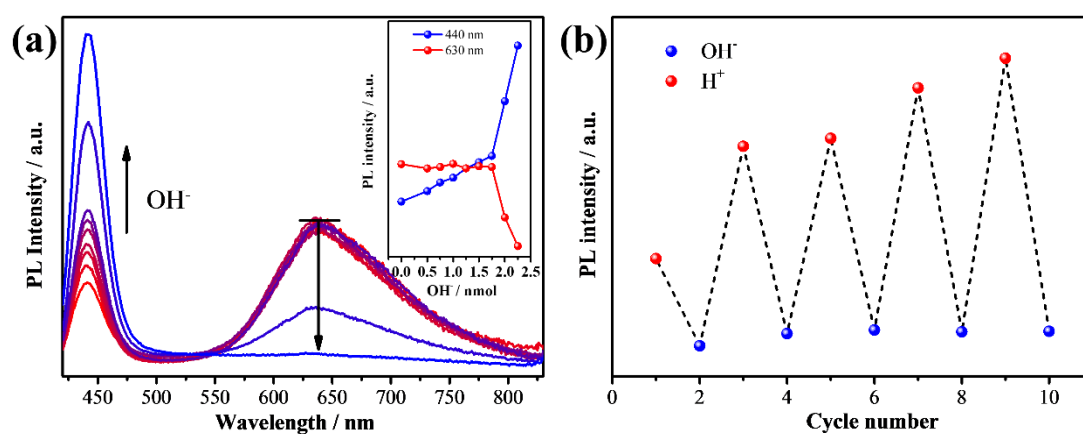


Figure 3. Photoluminescence spectra of as-synthesized $\text{Ag}_1\text{Au@DT}$ NCs after adding increasing amount of 50 mM NaOH aqueous solution, Fluorescence spectra were measured at $\lambda_{\text{ex}} = 320$ nm. The inset displays the relationship between photoluminescence (440 nm and 630 nm) intensity and the added mole amount of NaOH. (b) PL intensity of $\text{Ag}_1\text{Au@DT}$ NCs upon cyclic switching of the pH by adding 50 μl 50 mM NaOH and 50 μl 50 mM HCl aqueous solution.

Not only the dosing of Ag^+ , the environmental pH of $\text{Ag}_1\text{Au@DT}$ NCs also shows a prominent impact to the photoluminescence emission. Based on the reduction of HAuCl_4 precursors and complex interaction of Au(I)/Ag(I) with thiol groups (-SH) during the synthesis of metal NCs, the amount of H^+ in the stock solution can be precisely calculated to be 1.875 nmol (Equation 1 and 2, SI), so the solution of as made Au-Ag bimetallic NCs is acidic. Very interestingly, when varied amount of NaOH solution (0, 0.5, 0.75, 1.0, 1.25, 1.5, 1.75, 2.0 and 2.25 nmol) was added, the dual-emissive Au-Ag NCs exhibited unique ratiometric pH-dependent emissions (Fig. 3). As shown in Fig. 3a, if the added amount of OH^- (0~1.75 nmol) is less than the calculated value (1.875 nmol), the red emission at 630 nm is almost unchanged, whereas the blue one (440 nm) was slightly but linearly increased with the increasing amount OH^- . Once more NaOH solution was added (>1.875 nmol), *i.e.*, solution is basic, the dual emissions of Au-Ag NCs exhibited the opposite trend: the red emission dramatically reduced and almost quenched, while the blue emission precisely increased by two times, suggesting that the original red-emissive Au emitters

due to the strong coordination interaction of HO^- with Au induce the formation of the blue emitters because of Au/Ag molar ratio of 1:1 (Fig. 3a and inset). Besides, we observed that the blue and red emission can be reversibly recovered and quenched by a cycling titration of acid and base solution (Fig. 3b), respectively, indicating the meta-stability of luminous centers. Thus, as-synthesized $\text{Ag}_1\text{Au@DT}$ NCs could serve as potential ratiometric nanoprobe for pH sensing.

Nevertheless, the origin of dual-emission band for $\text{Ag}_x\text{Au@DT}$ NCs and its pH-dependent PL emission remains elusive. In most of case, the pH-dependent fluorescence properties was generally observed for ligand-protected metal NCs with AIE characteristic^[61-63], in which the pH value was deemed to alter the charge state of the protected ligand and inhibited the aggregation of the Au(I)-thiolate staple due to the electrostatic repulsion. In our case, the pH variation cannot be a trigger of AIE for $\text{Ag}_x\text{Au@DT}$ NCs because of the nonionic nature of alkylthiol (DT) protective ligands on the metal core surface. In the previous discussion, we precluded the possibility of PL emission due to the quantum size confinement effect of metal NCs, since the Ag^+ doping and pH variation did not change the structure of Au NCs core based on the characterizations of TEM and XPS (Fig. S2 and S3). Excitation spectrum of Au-Ag bimetal NCs gives more information on the nature of excited states of dual emissions (Fig. 4a). Unexpectedly, the long-wavelength red emission at 630 nm shows a broad excitation band centered at *ca.* 320 nm, and with an increase of Ag^+ dosing, its excitation intensity is gradually decreased and finally completely disappears, consistent with the evolution of PL emission (Fig. 1b); while the short-wavelength blue emission at 440 nm exhibits a long-wavelength excitation centered at 390 nm. Similar excited state energy levels with just 0.70 eV energetic gap answers the strong energy transfer between two emission centers of Au-Ag bimetal NCs (Fig. 1a), which also precludes the LMCT and/or LMMCT model of ligand to metal (or metal NCs) charge transfer for the contribution of PL emission with much higher theoretical energy levels.^[64]

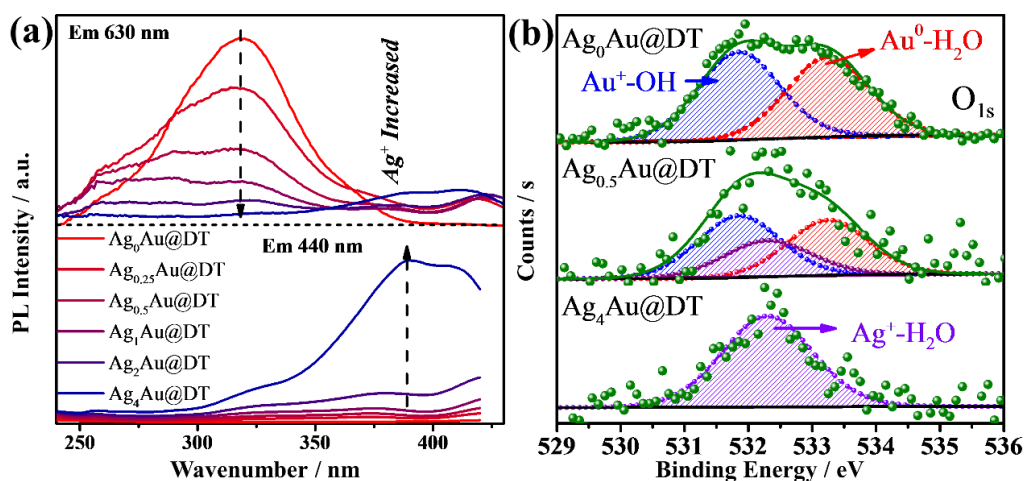


Figure 4. Excitation spectra (a) of $\text{Ag}_x\text{Au@DT}$ NCs and XPS spectrum (b) of O 1s for $\text{Ag}_0\text{Au@DT}$ and $\text{Ag}_{0.5}\text{Au@DT}$ and $\text{Ag}_4\text{Au@DT}$ NCs.

Very recently, after long-term and systematic investigation, using a combined experimental and computational approach, in particular with the help of steady and ultra-fast absorption and emission spectra, we unambiguously confirmed the existence of new interface states due to the spatial overlapping of p orbitals of oxygen atoms of structural water molecules (SWs) at the confined nanointerface of soft and hard nanocavity.^[57, 58, 64-71] It is called the p band intermediate state (PBIS) with π bonding features, which not only provides an ensemble of intermediate states

for bright photoluminescence (PL) emission, but also acts as an alternative reaction channel for static electron transfer.^[69-71] Considering the ubiquitous properties of structural water molecules (SWs) at heterogeneous interface and the universality of our PBIS model, we performed the XPS measurement of O_{1s} to test the presence of species of SWs for three typical metal NCs of Ag₀Au@DT and Ag_{0.5}Au@DT and Ag₄Au@DT NCs (Fig. 4b). As expectedly, mono-metal Ag₀Au@DT NCs show two distinct binding energies at 531.8 eV and 533.2 eV with molar ratio close to 1:1 (Fig. 4b, top and Tab. S3), which was assigned to hydroxide and water molecules chemically adsorbed on the Au(I) ion and Au atoms, respectively, indicating the presence of SWs {OH·H₂O} at the metal core surface (Fig. 5b). With the increase of Ag⁺ dosing in the synthesis, the content of SWs interacted with Au atoms was significantly decreased, while a new chemically adsorbed specie containing O atoms of Ag_{0.5}Au@DT was produced at 532.3 eV, which was assigned to water coordinated with Ag⁺ (Fig. 4b, middle). If the Au core was completely covered by a thiolate-Ag⁺ motif shell, only Ag⁺-H₂O complexes were observed at 532.3 eV (Fig. 4b, bottom and Fig. 5c).

Importantly, it is worth noting that, after the vacuum evacuation or ice-drying, due to the removing of SWs with weak interactions (Fig. 5c), the blue emission at 440 nm of Ag₄Au@DT NCs was quenched. If trace amount of water was re-added, the blue emission could be recovered (not shown here). This probably answers that, Ag₄Au@DT NCs only captured one signal of chemically adsorbed water molecules with Ag⁺ at 532.3 eV owing to high vacuum treatment during the XPS measurement, indicating the blue emissive SWs are weakly bonded on the fully core-shell structured Au-Ag bimetal Au NCs though water bridge which strongly coordinated with Ag⁺ (Fig. 5c). Thus, PL properties strongly depend on the binding mode of SWs. Only the SWs with medium binding strength to metal emit the long-wavelength emission, while the SWs strongly coordinated with metals do not emit the color due to the limitation of spatial configuration of p orbitals of O atoms in the SWs, eg., {Ag⁺·H₂O} dimers, but weakly bound SWs by hydrogen-Bonding on the {Ag⁺·H₂O} dimers could emit the short-wavelength blue emission (Fig. 5c). This also answers the origin of unique ratiometric pH-dependent dual-emissions (Fig. 3). At acid conditions, the hydroxide adsorbed on the Au-Ag bimetal NCs was neutralized, only red-emission was observed. At basic conditions, the first layer of SWs weakly interacted with Au(I) and Au(0) were replaced by hydroxide groups with stronger coordination ability to metals, which can be used as new immobilized sites for hosting SWs with weak interaction by H-bonding interaction (the blue emissive SWs with less stability), consequently the blue emission was intensified (Fig. 3a). obviously, the overlapping degree of two O atoms in the varied SWs, *ie.*, the stability of two type of SWs as emitters, determines the abnormal relation of long-wavelength emission with short-wavelength excitation (Fig. 4a and Fig. 5) and their varied lifetimes of dual-emissions (Fig. 1d). The presence of SWs with the varied stability and multiple intermediate states at nanoscale interface probably answers the promoting role of alkali metal ion in both electro-catalytic reaction of HER and ORR and water-gas shift reaction (WGSR) by providing the alternative channels for concerted proton and electron transfer.^[69-71]

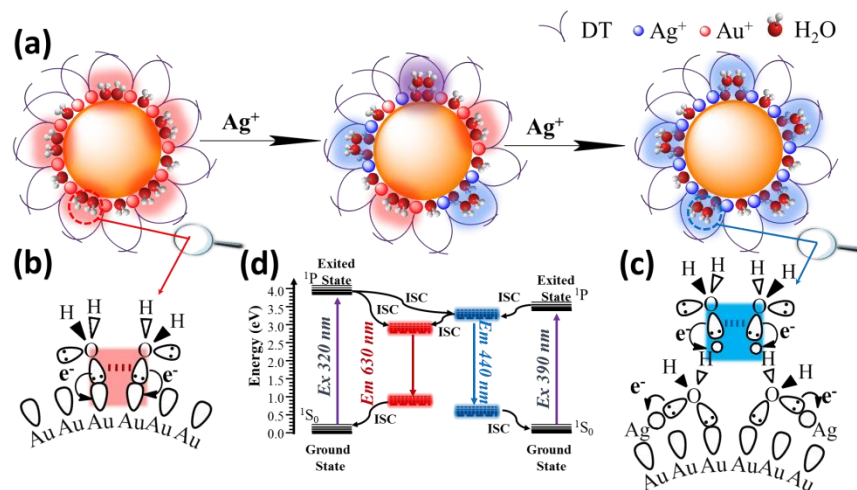


Figure 5. Schematic illustration of structural water molecules (SWs) confined at nanoscale interface of Au-Ag bimetal NCs packed by protective ligands emit bright dual-photoluminescence (a), the red emissive SWs strongly binding on the single metal Au NCs (b), the blue emissive SWs weakly binding on the fully core-shell structured Au-Ag bimetal Au NCs though water bridge which strongly coordinated with Ag^+ (c), and energy diagram of dual emissions of Au-Ag bimetal NCs.

The diagnostic experiments through dosing with S^{2-} anions (Fig. S4), the blue emission of $\text{Ag}_1\text{Au}@$ DT NCs was gradually quenched with the increasing dosing amount S^{2-} due to its strong capacity to precipitate Ag^+ . Obviously, the removal of surface Ag^+ induce the losing of SWs confined on the thiolate- Ag^+ motifs, resulting in the quenching of blue emissions. Even though the red-emission was also reduced, its emission also could be easily distinguished due to relative strong affinity of SWs with Au(I) and Au(0) (Fig. S4 and inset). The weakening of red-emission probably is attributed to the covering of emitters due to the deposition of AgS precipitates. Indeed, the surface thiol ligand plays a role to create the nano-microenvironment with hydrophobicity for hosting the SWs. This was verified by changing the DT concentration during synthesis to influence the dual-emissions (Fig. S5). At low concentration of DT ligands (less than 2.0 equivalent to metal), the dual-emissions were hardly distinguished (Fig. S6, inset). Only above this critical value, the dual-emissions of Ag-Ag bimetal NCs were boosted with more feeding of DT molecules since the dense packing of DT on the metal core creates more hydrophobic environment, which strengthen the stability of SWs (or stronger overlapping of p orbitals of O atoms by space interactions). Thus, we clearly addressed that, the emitter of dual-emissive Au-Ag bimetal NCs are coming from the SWs with varied stability (Fig. 5b and 5c), instead of metal NCs or AIE of surface protective ligands^[46, 72].

If we consider SWs confined at nanoscale interface as emitters, the reported abnormal PL properties of metal NCs could be easily elucidated, including solvent effect, pH-dependent behavior, surface ligand effect, multiple emitter centers, large-Stoke's shift, ^[12, 57, 66, 67, 73-83]. Herein, using our theory, taken an example of abnormal anti-galvanic replacement reaction approach for the synthesis of thiolate-protected Ag-Au NCs could be easily explained.^[41, 42] Classical galvanic replacement reaction involves the spontaneous reduction of a noble-metal cationic by a less noble metal in solution driven by the difference in redox potentials ($\text{Ag} + \text{Au}^+ \rightarrow \text{Ag}^+ + \text{Au}$),^[40, 45] while the anti-galvanic replacement reaction means an inverse process ($\text{Ag}^+ + \text{Au} \rightarrow \text{Ag} + \text{Au}^+$), which really subverted our traditional cognitive way. But, the

intermediate states formed by SWs with the overlapping of p orbitals of O atoms provide the alternative channels for the reverse electron transfer between Au and Ag⁺, thus the anti-galvanic replacement reaction was observed.^[84-86] The discovery of these dynamic interface states also provides a completely new insight to understand the nature of heterogeneous catalysis and/or interface state (bonding), beyond the conventional metal-centered d band theory.^[69-71, 87, 88]

Conclusion

In summary, bimetallic Ag-Au@DT NCs with well-resolved dual-emission (440 nm and 630 nm) were successfully achieved through a facial one-pot approach. The newly boosted blue emission is the consequence of the doping of silver atom as Ag(I)-thiolate into the staple motif site of Au NCs, which is confirmed by the XPS and TEM characterization. Very interestingly, Ag₁Au@DT NCs can sense a reversible dual-emission signal changes in the environmental pH, which enabled it as a potential ratiometric nanoprobe for pH sensing. The combined characterizations of absorption, excitation and emission spectrum confirm that, the true emitters of dual-emission of Ag₁Au@DT NCs are structural water molecules (SWs) confined on the surface of metal NCs core with varied stability. This answer the PL properties of metal NCs are extremely susceptible to the surrounding microenvironments of SWs, such as the dosing of Ag⁺, pH, and packing mode of surface ligands. Since the adsorption of SWs at nanoscale interface is a ubiquitous phenomenon in nature, the concept of 'SWs as emitters' could be used as a based modal to elucidate the origin of PL of other low-dimensioned quantum dots, such as carbon, semiconductor and perovskites type materials. In addition, the concept of 'surface electronic states' formed by space overlapping of p orbitals of O atoms in SWS, could act as an alternative channel for concerted electron and proton transfer, which provide new insights to in-depth understanding of heterogeneous catalysis and/or the nature of interface states (or interfacial bondings).^[57, 69-71]

Acknowledgments: This research was funded by the NSFC (21872053 and 21573074), the Science and Technology Commission of Shanghai Municipality (19520711400), the Open Project Program of Academician and Expert Workstation, Shanghai Curui Low-Carbon Energy Technology Co., Ltd., the JORISS program, and the Postdoctoral Science Foundation of China (2018M640360). K.Z. thanks ENS de Lyon for a temporary position as an invited professor in France.

References

- [1] T.G. Schaaff, M.N. Shafiqullin, J.T. Khoury, I. Vezmar, R.L. Whetten, W.G. Cullen, P.N. First, Isolation of Smaller Nanocrystal Au Molecules: Robust Quantum Effects in Optical Spectra, *J. Phys. Chem. B*, 101 (1997) 7885-7891.
- [2] D. Lee, R.L. Donkers, G. Wang, A.S. Harper, R.W. Murray, Electrochemistry and Optical Absorbance and Luminescence of Molecule-like Au₃₈ Nanoparticles, *J. Am. Chem. Soc.*, 126 (2004) 6193-6199.
- [3] Y. Negishi, K. Nobusada, T. Tsukuda, Glutathione-Protected Gold Clusters Revisited: Bridging the Gap between Gold(I)-Thiolate Complexes and Thiolate-Protected Gold Nanocrystals, *J. Am. Chem. Soc.*, 127 (2005) 5261-5270.
- [4] M. Walter, J. Akola, O. Lopez-Acevedo, P.D. Jadzinsky, G. Calero, C.J. Ackerson, R.L. Whetten, H. Grönbeck, H. Häkkinen, A unified view of ligand-protected gold clusters as superatom complexes, *Proc. Natl. Acad. Sci. USA*, 105 (2008) 9157-9162.
- [5] M. Zhu, C.M. Aikens, F.J. Hollander, G.C. Schatz, R. Jin, Correlating the Crystal Structure of A Thiol-Protected Au₂₅ Cluster and Optical Properties, *J. Am. Chem. Soc.*, 130 (2008) 5883-5885.
- [6] I. Chakraborty, T. Pradeep, Atomically Precise Clusters of Noble Metals: Emerging Link between

- Atoms and Nanoparticles, *Chem. Rev.*, 117 (2017) 8208-8271.
- [7] F. Bertorelle, I. Russier-Antoine, N. Calin, C. Comby-Zerbino, A. Bensalah-Ledoux, S. Guy, P. Dugourd, P.F. Brevet, Z. Sanader, M. Krstic, V. Bonacic-Koutecky, R. Antoine, Au₁₀(SG)₁₀: A Chiral Gold Catenane Nanocluster with Zero Confined Electrons. Optical Properties and First-Principles Theoretical Analysis, *J. Phys. Chem. Lett.*, 8 (2017) 1979-1985.
- [8] I. Russier-Antoine, F. Bertorelle, M. Vojkovic, D. Rayane, E. Salmon, C. Jonin, P. Dugourd, R. Antoine, P.F. Brevet, Non-linear optical properties of gold quantum clusters. The smaller the better, *Nanoscale*, 6 (2014) 13572-13578.
- [9] J. Zheng, C. Zhang, R.M. Dickson, Highly fluorescent, water-soluble, size-tunable gold quantum dots, *Phys. Rev. Lett.*, 93 (2004) 077402.
- [10] J. Zheng, P.R. Nicovich, R.M. Dickson, Highly fluorescent noble-metal quantum dots, *Annu. Rev. Phys. Chem.*, 58 (2007) 409-431.
- [11] J. Xie, Y. Zheng, J.Y. Ying, Protein-Directed Synthesis of Highly Fluorescent Gold Nanoclusters, *J. Am. Chem. Soc.*, 131 (2009) 888-889.
- [12] Z. Luo, X. Yuan, Y. Yu, Q. Zhang, D.T. Leong, J.Y. Lee, J. Xie, From aggregation-induced emission of Au(I)-thiolate complexes to ultrabright Au(0)@Au(I)-thiolate core-shell nanoclusters, *J. Am. Chem. Soc.*, 134 (2012) 16662-16670.
- [13] B. Musnier, K.D. Wegner, C. Comby-Zerbino, V. Trouillet, M. Jourdan, I. Hausler, R. Antoine, J.L. Coll, U. Resch-Genger, X. Le Guevel, High photoluminescence of shortwave infrared-emitting anisotropic surface charged gold nanoclusters, *Nanoscale*, 11 (2019) 12092-12096.
- [14] H. Tsunoyama, N. Ichikuni, H. Sakurai, T. Tsukuda, Effect of Electronic Structures of Au Clusters Stabilized by Poly(N-vinyl-2-pyrrolidone) on Aerobic Oxidation Catalysis, *J. Am. Chem. Soc.*, 131 (2009) 7086-7093.
- [15] J. Li, R.R. Nasaruddin, Y. Feng, J. Yang, N. Yan, J. Xie, Tuning the Accessibility and Activity of Au₂₅(SR)₁₈ Nanocluster Catalysts through Ligand Engineering, *Chem. Eur. J.*, 22 (2016) 14816-14820.
- [16] X. Cai, G. Saranya, K. Shen, M. Chen, R. Si, W. Ding, Y. Zhu, Reversible Switching of Catalytic Activity by Shuttling an Atom into and out of Gold Nanoclusters, *Angew. Chem. Int. Ed.*, 58 (2019,) 9964-9968.
- [17] D. Yang, W. Pei, S. Zhou, J. Zhao, W. Ding, Y. Zhu, Controllable Conversion of CO₂ on Non-Metallic Gold Clusters, *Angew. Chem. Int. Ed.*, 59 (2020) 1919-1924.
- [18] G. Li, X. Sui, X. Cai, W. Hu, X. Liu, M. Chen, Y. Zhu, Precisely Constructed Silver Active Sites in Gold Nanoclusters for Chemical Fixation of CO₂, *Angew. Chem. Int. Ed.*, 60 (2021) 10573-10576.
- [19] X. Cai, W. Hu, S. Xu, D. Yang, M. Chen, M. Shu, R. Si, W. Ding, Y. Zhu, Structural Relaxation Enabled by Internal Vacancy Available in a 24-Atom Gold Cluster Reinforces Catalytic Reactivity, *J. Am. Chem. Soc.*, 142 (2020) 4141-4153.
- [20] Y. Zhu, H. Qian, M. Zhu, R. Jin, Thiolate-protected Au(n) nanoclusters as catalysts for selective oxidation and hydrogenation processes, *Adv. Mater.*, 22 (2010) 1915-1920.
- [21] R. Jin, Quantum sized, thiolate-protected gold nanoclusters, *Nanoscale*, 2 (2010) 343-362.
- [22] I. Diez, R.H. Ras, Fluorescent silver nanoclusters, *Nanoscale*, 3 (2011) 1963-1970.
- [23] J. Zheng, C. Zhou, M. Yu, J. Liu, Different sized luminescent gold nanoparticles, *Nanoscale*, 4 (2012) 4073-4083.
- [24] Z. Luo, K. Zheng, J. Xie, Engineering ultrasmall water-soluble gold and silver nanoclusters for biomedical applications, *Chem. Commun.*, 50 (2014) 5143-5155.
- [25] J. Sun, Y. Jin, Fluorescent Au nanoclusters: recent progress and sensing applications, *J. Mater.*

Chem. C, 2 (2014) 8000-8011.

- [26] R. Jin, C. Zeng, M. Zhou, Y. Chen, Atomically Precise Colloidal Metal Nanoclusters and Nanoparticles: Fundamentals and Opportunities, *Chem. Rev.*, 116 (2016) 10346-10413.
- [27] V. Bonacic-Koutecky, A. Kulesza, L. Gell, R. Mitric, R. Antoine, F. Bertorelle, R. Hamouda, D. Rayane, M. Broyer, T. Tabarin, P. Dugourd, Silver cluster-biomolecule hybrids: from basics towards sensors, *Phys. Chem. Chem. Phys.*, 14 (2012) 9282-9290.
- [28] Z. Lei, X.K. Wan, S.F. Yuan, Z.J. Guan, Q.M. Wang, Alkynyl Approach toward the Protection of Metal Nanoclusters, *Acc. Chem. Res.*, 51 (2018) 2465-2474.
- [29] J. Yan, B.K. Teo, N. Zheng, Surface Chemistry of Atomically Precise Coinage-Metal Nanoclusters: From Structural Control to Surface Reactivity and Catalysis, *Acc. Chem. Res.*, 51 (2018) 3084-3093.
- [30] S. Wang, X. Meng, A. Das, T. Li, Y. Song, T. Cao, X. Zhu, M. Zhu, R. Jin, A 200-fold quantum yield boost in the photoluminescence of silver-doped Ag(x)Au(25-x) nanoclusters: the 13th silver atom matters, *Angew. Chem. Int. Ed.*, 53 (2014) 2376-2380.
- [31] Z. Wu, Y. Du, J. Liu, Q. Yao, T. Chen, Y. Cao, H. Zhang, J. Xie, Auophilic Interactions in the Self-Assembly of Gold Nanoclusters into Nanoribbons with Enhanced Luminescence, *Angew. Chem. Int. Ed.*, 58 (2019) 8139-8144.
- [32] P.D. Jadzinsky, G. Calero, C.J. Ackerson, D.A. Bushnell, R.D. Kornberg, Structure of a Thiol Monolayer-Protected Gold Nanoparticle at 1.1 Å Resolution, *Science*, 318 (2007) 430-433.
- [33] H. Hirai, S. Ito, S. Takano, K. Koyasu, T. Tsukuda, Ligand-protected gold/silver superatoms: current status and emerging trends, *Chem. Sci.*, 11 (2020) 12233-12248.
- [34] X. Kang, Y. Li, M. Zhu, R. Jin, Atomically precise alloy nanoclusters: syntheses, structures, and properties, *Chem. Soc. Rev.*, 49 (2020) 6443-6514.
- [35] Y. Negishi, T. Iwai, M. Ide, Continuous modulation of electronic structure of stable thiolate-protected Au₂₅ cluster by Ag doping, *Chem. Commun.*, 46 (2010) 4713-4715.
- [36] C. Kumara, A. Dass, (AuAg)₁₄₄(SR)₆₀ alloy nanomolecules, *Nanoscale*, 3 (2011) 3064-3067.
- [37] C. Kumara, A. Dass, AuAg alloy nanomolecules with 38 metal atoms, *Nanoscale*, 4 (2012) 4084-4086.
- [38] X. Dou, X. Yuan, Q. Yao, Z. Luo, K. Zheng, J. Xie, Facile synthesis of water-soluble Au(25-x)Ag(x) nanoclusters protected by mono- and bi-thiolate ligands, *Chem. Commun.*, 50 (2014) 7459-7462.
- [39] Y. Yu, Q. Yao, T. Chen, G.X. Lim, J. Xie, The Innermost Three Gold Atoms Are Indispensable To Maintain the Structure of the Au₁₈(SR)₁₄ Cluster, *J. Phys. Chem. C*, 120 (2016) 22096-22102.
- [40] T. Udayabhaskararao, Y. Sun, N. Goswami, S.K. Pal, K. Balasubramanian, T. Pradeep, Ag₇Au₆: a 13-atom alloy quantum cluster, *Angew. Chem. Int. Ed.*, 51 (2012) 2155-2159.
- [41] J.-P. Choi, C. A. Fields-Zinna, R.L. Stiles, R. Balasubramanian, A.D. Douglas, M.C. Crowe, R.W. Murray, Reactivity of [Au₂₅(SCH₂CH₂Ph)₁₈]¹⁻ Nanoparticles with Metal Ions, *J. Phys. Chem. C*, 114 (2010) 15890-15896.
- [42] Z. Wu, Anti-galvanic reduction of thiolate-protected gold and silver nanoparticles, *Angew. Chem. Int. Ed.*, 51 (2012) 2934-2938.
- [43] H. Hirai, S. Takano, T. Tsukuda, Synthesis of Trimetallic (HPd@M₂Au₈)(³⁺) Superatoms (M = Ag, Cu) via Hydride-Mediated Regioselective Doping to (Pd@Au₈)(²⁺), *ACS omega*, 4 (2019) 7070-7075.
- [44] S. Takano, H. Hirai, S. Muramatsu, T. Tsukuda, Hydride-Mediated Controlled Growth of a Bimetallic (Pd@Au₈)(²⁺) Superatom to a Hydride-Doped (HPd@Au₁₀)(³⁺) Superatom, *J. Am. Chem. Soc.*, 140 (2018) 12314-12317.
- [45] Z. Gan, N. Xia, Z. Wu, Discovery, Mechanism, and Application of Antigalvanic Reaction, *Acc. Chem.*

Res., 51 (2018) 2774-2783.

[46] X. Dou, X. Yuan, Y. Yu, Z. Luo, Q. Yao, D.T. Leong, J. Xie, Lighting up thiolated Au@Ag nanoclusters via aggregation-induced emission, *Nanoscale*, 6 (2014) 157-161.

[47] W. Zhou, Y. Fang, J. Ren, S. Dong, DNA-templated silver and silver-based bimetallic clusters with remarkable and sequence-related catalytic activity toward 4-nitrophenol reduction, *Chem. Commun.*, 55 (2019) 373-376.

[48] W. Li, C. Liu, H. Abroshan, Q. Ge, X. Yang, H. Xu, G. Li, Catalytic CO Oxidation Using Bimetallic MxAu_{25-x} Clusters: A Combined Experimental and Computational Study on Doping Effects, *J. Phys. Chem. C*, 120 (2016) 10261-10267.

[49] T. Ye, X. An, Synthesis and properties of Au–Ag bimetallic nanoclusters with dual-wavelength emission, *New J. Chem.*, 43 (2019) 569-572.

[50] J. Jana, T. Aditya, T. Pal, Achievement of silver-directed enhanced photophysical properties of gold nanoclusters, *New J. Chem.*, 43 (2019) 7074-7082.

[51] X. Liu, J. Yuan, C. Yao, J. Chen, L. Li, X. Bao, J. Yang, Z. Wu, Crystal and Solution Photoluminescence of MAg₂₄(SR)₁₈ (M = Ag/Pd/Pt/Au) Nanoclusters and Some Implications for the Photoluminescence Mechanisms, *J. phys. Chem. C*, 121 (2017) 13848-13853.

[52] C. Yao, J. Chen, M.B. Li, L. Liu, J. Yang, Z. Wu, Adding two active silver atoms on Au(2)(5) nanoparticle, *Nano Lett.*, 15 (2015) 1281-1287.

[53] Q. Yuan, X. Kang, D. Hu, C. Qin, S. Wang, M. Zhu, Metal synergistic effect on cluster optical properties: based on Ag₂₅ series nanoclusters, *Dalton Trans.*, 48 (2019) 13190-13196.

[54] Y. Xiao, J. Zhou, M. Chen, W. Wen, X. Zhang, S. Wang, Modulation of the optical color of Au nanoclusters and its application in ratiometric photoluminescence detection, *Chem. Commun.*, 54 (2018) 10467-10470.

[55] F. Liu, T. Bing, D. Shangguan, M. Zhao, N. Shao, Ratiometric Fluorescent Biosensing of Hydrogen Peroxide and Hydroxyl Radical in Living Cells with Lysozyme-Silver Nanoclusters: Lysozyme as Stabilizing Ligand and Fluorescence Signal Unit, *Anal. Chem.*, 88 (2016) 10631-10638.

[56] X. Huang, J. Song, B.C. Yung, X. Huang, Y. Xiong, X. Chen, Ratiometric optical nanoprobe enable accurate molecular detection and imaging, *Chem. Soc. Rev.*, 47 (2018) 2873-2920.

[57] X.-D. Hu, T.-Q. Yang, B.-Q. Shan, B. Peng, K. Zhang, Topological excitation of singly hydrated hydroxide complex in confined sub-nanospace for bright color emission and heterogeneous catalysis, *ChemRxiv*, DOI: 10.26434/chemrxiv.13107548.v1 (2020).

[58] T.-Q. Yang, Bo-Peng, J.-F. Zhou, B.-Q. Shan, K. Zhang, Hydrogen-Bonded Water Clusters Confined in Nanocavity as Bright Color Emitters, *ChemRxiv*, DOI: 10.26434/chemrxiv.12927452.v1 (2020).

[59] C. Zhou, C. Sun, M. Yu, Y. Qin, J. Wang, M. Kim, J. Zheng, Luminescent Gold Nanoparticles with Mixed Valence States Generated from Dissociation of Polymeric Au(I) Thiolates, *J. Phys. Chem. C*, 114 (2010) 7727–7732.

[60] X. Yuan, M.I. Setyawati, A.S. Tan, C.N. Ong, D.T. Leong, J. Xie, Highly luminescent silver nanoclusters with tunable emissions: cyclic reduction–decomposition synthesis and antimicrobial properties, *NPG Asia Materials*, 5 (2013) e39-e39.

[61] M. Wu, J. Zhao, D.M. Chevrier, P. Zhang, L. Liu, Luminescent Au(I)–Thiolate Complexes through Aggregation-Induced Emission: The Effect of pH during and Post Synthesis, *J. Phys. Chem. C*, 123 (2019) 6010-6017.

[62] H.Y. Chang, Y.T. Tseng, Z. Yuan, H.L. Chou, C.H. Chen, B.J. Hwang, M.C. Tsai, H.T. Chang, C.C. Huang, The effect of ligand-ligand interactions on the formation of photoluminescent gold nanoclusters

- embedded in Au(i)-thiolate supramolecules, *Phys. Chem. Chem. Phys.*, **19** (2017) 12085-12093.
- [63] X. Su, J. Liu, pH-Guided Self-Assembly of Copper Nanoclusters with Aggregation-Induced Emission, *ACS Appl. Mater. Interfaces*, **9** (2017) 3902-3910.
- [64] T. Yang, B. Shan, F. Huang, S. Yang, B. Peng, E. Yuan, P. Wu, K. Zhang, P band intermediate state (PBIS) tailors photoluminescence emission at confined nanoscale interface, *Commun. Chem.*, **2** (2019) 132.
- [65] Y. Chen, T. Yang, H. Pan, Y. Yuan, L. Chen, M. Liu, K. Zhang, S. Zhang, P. Wu, J. Xu, Photoemission mechanism of water-soluble silver nanoclusters: ligand-to-metal-metal charge transfer vs strong coupling between surface plasmon and emitters, *J. Am. Chem. Soc.*, **136** (2014) 1686-1689.
- [66] T. Yang, S. Dai, S. Yang, L. Chen, P. Liu, K. Dong, J. Zhou, Y. Chen, H. Pan, S. Zhang, J. Chen, K. Zhang, P. Wu, J. Xu, Interfacial Clustering-Triggered Fluorescence–Phosphorescence Dual Solvoluminescence of Metal Nanoclusters, *J. Phys. Chem. Lett.*, **8** (2017) 3980-3985.
- [67] T. Yang, S. Dai, H. Tan, Y. Zong, Y. Liu, J. Chen, K. Zhang, P. Wu, S. Zhang, J. Xu, Y. Tian, Mechanism of Photoluminescence in Ag Nanoclusters: Metal-Centered Emission versus Synergistic Effect in Ligand-Centered Emission, *J. Phys. Chem. C*, **123** (2019) 18638-18645.
- [68] T.-Q. Yang, T.-Y. Ning, B. Peng, B.-Q. Shan, Y.-X. Zong, P. Hao, E.-H. Yuan, Q.-M. Chen, K. Zhang, Interfacial electron transfer promotes photo-catalytic reduction of 4-nitrophenol by Au/Ag₂O nanoparticles confined in dendritic mesoporous silica nanospheres, *Catal. Sci. Technol.*, **9** (2019) 5786-5792.
- [69] X.-D. Hu, B.-Q. Shan, R. Tao, T.-Q. Yang, K. Zhang, Interfacial Hydroxyl Promotes the Reduction of 4-Nitrophenol by Ag-based Catalysts Confined in Dendritic Mesoporous Silica Nanospheres, *J. Phys. Chem. C*, **125** (2021) 2446-2453.
- [70] B.Q. Shan, J.F. Zhou, M. Ding, X.D. Hu, K. Zhang, Surface electronic states mediate concerted electron and proton transfer at metal nanoscale interfaces for catalytic hydride reduction of -NO₂ to -NH₂, *Phys. Chem. Chem. Phys.*, **23** (2021) 12950-12957,.
- [71] R. Tao, B.-Q. Shan, H.-D. Sun, M. Ding, Q.-S. Xue, J.-G. Jiang, P. Wu, K. Zhang, Surface Molecule Manipulated Pt/TiO₂ Catalysts for Selective Hydrogenation of Cinnamaldehyde, *J. Phys. Chem. C*, **125** (2021) 13304-13312.
- [72] Z. Wu, Q. Yao, O. Jin, H. Chai, N. Ding, W. Xu, S. Zang, J. Xie, Unraveling the Impact of Gold(I)–Thiolate Motifs on the Aggregation-Induced Emission of Gold Nanoclusters, *Angew. Chem. Int. Ed.*, **59** (2020) 9934–9939.
- [73] Z. Wu, R. Jin, On the ligand's role in the fluorescence of gold nanoclusters, *Nano Lett.*, **10** (2010) 2568-2573.
- [74] X. Jia, J. Li, E. Wang, Supramolecular self-assembly of morphology-dependent luminescent Ag nanoclusters, *Chem. Commun.*, **50** (2014) 9565-9568.
- [75] Z. Wu, J. Liu, Y. Gao, H. Liu, T. Li, H. Zou, Z. Wang, K. Zhang, Y. Wang, H. Zhang, B. Yang, Assembly-Induced Enhancement of Cu Nanoclusters Luminescence with Mechanochromic Property, *J. Am. Chem. Soc.*, **137** (2015) 12906-12913.
- [76] L.G. AbdulHalim, N. Kothalawala, L. Sinatra, A. Dass, O.M. Bakr, Neat and complete: thiolate-ligand exchange on a silver molecular nanoparticle, *J. Am. Chem. Soc.*, **136** (2014) 15865-15868.
- [77] I. Díez, M.I. Kanyuk, A.P. Demchenko, A. Walther, H. Jiang, O. Ikkala, R.H. Ras, Blue, green and red emissive silver nanoclusters formed in organic solvents, *Nanoscale*, **4** (2012) 4434-4437.
- [78] G.D. Cremer, E. Coutiño-Gonzalez, M.B.J. Roeffaers, B. Moens, J. Ollevier, M.V.d. Auweraer, R.

- Schoonheydt, P.A. Jacobs, F.C.D. Schryver, J. Hofkens, D.E.D. Vos, B.F. Sels, T. Vosch, Characterization of Fluorescence in Heat-Treated Silver-Exchanged Zeolites, *J. Am. Chem. Soc.*, 131 (2009) 3049-3056.
- [79] O. Fenwick, E. Coutiño-Gonzalez, D. Grandjean, W. Baekelant, F. Richard, S. Bonacchi, D. De Vos, P. Lievens, M. Roeffaers, J. Hofkens, P. Samorì, Tuning the energetics and tailoring the optical properties of silver clusters confined in zeolites, *Nat. Mater.*, 15 (2016) 1017-1022.
- [80] D. Grandjean, E. Coutiño-Gonzalez, N.T. Cuong, E. Fron, W. Baekelant, S. Aghakhani, P. Schlexer, F. D'Acapito, D. Banerjee, M.B.J. Roeffaers, M.T. Nguyen, J. Hofkens, P. Lievens, Origin of the bright photoluminescence of few-atom silver clusters confined in LTA zeolites, *Science*, (2018).
- [81] H. Lin, K. Imakita, M. Fujii, Reversible emission evolution from Ag activated zeolite Na-A upon dehydration/hydration, *Appl. Phys. Lett.*, 105 (2014) 211903.
- [82] S. Aghakhani, D. Grandjean, W. Baekelant, E. Coutiño-Gonzalez, E. Fron, K. Kvashnina, M.B.J. Roeffaers, J. Hofkens, B.F. Sels, P. Lievens, Atomic scale reversible opto-structural switching of few atom luminescent silver clusters confined in LTA zeolites, *Nanoscale*, 10 (2018) 11467-11476.
- [83] E. Coutiño-Gonzalez, W. Baekelant, D. Grandjean, M.B.J. Roeffaers, E. Fron, M.S. Aghakhani, N. Bovet, M. Van der Auweraer, P. Lievens, T. Vosch, B. Sels, J. Hofkens, Thermally activated LTA(Li)-Ag zeolites with water-responsive photoluminescence properties, *J. Mater. Chem. C*, 3 (2015) 11857-11867.
- [84] M. Cammarata, S. Zerdane, L. Balducci, G. Azzolina, S. Mazerat, C. Exertier, M. Trabuco, M. Levantino, R. Alonso-Mori, J.M. Glowina, S. Song, L. Catala, T. Mallah, S.F. Matar, E. Collet, Charge transfer driven by ultrafast spin transition in a CoFe Prussian blue analogue, *Nat. Chem.*, 13 (2021) 10-14.
- [85] C.Q. Jiao, Y.S. Meng, Y. Yu, W.J. Jiang, W. Wen, H. Oshio, Y. Luo, C.Y. Duan, T. Liu, Effect of Intermolecular Interactions on Metal-to-Metal Charge Transfer: A Combined Experimental and Theoretical Investigation, *Angew. Chem. Int. Ed.*, 58 (2019) 17009-17015.
- [86] I.-R. Jeon, S. Calancea, A. Panja, D.M. Piñero Cruz, E.S. Koumoussi, P. Dechambenoit, C. Coulon, A. Wattiaux, P. Rosa, C. Mathonière, R. Clérac, Spin crossover or intra-molecular electron transfer in a cyanido-bridged Fe/Co dinuclear dumbbell: a matter of state, *Chem. Sci.*, 4 (2013) 2463.
- [87] A.J. Medford, A. Vojvodic, J.S. Hummelshøj, J. Voss, F. Abild-Pedersen, F. Studt, T. Bligaard, A. Nilsson, J.K. Nørskov, From the Sabatier principle to a predictive theory of transition-metal heterogeneous catalysis, *Journal of Catalysis*, 328 (2015) 36-42.
- [88] T. Liu, M. Guo, A. Orthaber, R. Lomoth, M. Lundberg, S. Ott, L. Hammarstrom, Accelerating proton-coupled electron transfer of metal hydrides in catalyst model reactions, *Nat. Chem.*, 10 (2018) 881-887.

Supporting information

Silver cation-mediated dual-emissive Au–Ag bimetallic nanoclusters for pH ratiometric sensing

Bo Peng,^a Liu-Xi Zheng,^a Pan-Yue Wang,^a Jia-Feng Zhou,^a Meng Ding,^a Hao-Di Sun,^a Bing-Qian Shan*^a, Kun Zhang*^{a,b,c}

^aShanghai Key Laboratory of Green Chemistry and Chemical Processes, College of Chemistry and Molecular Engineering, East China Normal University, Shanghai 200062, China;

^bLaboratoire de chimie, Ecole Normale Supérieure de Lyon, Institut de Chimie de Lyon, Université de Lyon, 46 Allée d'Italie, 69364 Lyon cedex 07, France;

^cShandong Provincial Key Laboratory of Chemical Energy Storage and Novel Cell Technology, School of Chemistry and Chemical Engineering, Liaocheng University, Liaocheng, 252059, Shandong, P. R. China

* Correspondence: bqshan_ecnu@163.com and kzhang@chem.ecnu.edu.cn (K.Z.)

Experimental section

Materials

All reagents used were purchased from Sinopharm Chemical Reagent Co., Ltd. except Glutathione in the reduced form (GSH), which was purchased from Aladdin (Shanghai, China). All chemicals were used as received without any further purification. Deionized water was used in all experiments.

Synthesis of Ag_xAu@DT NCs with different ratio of Ag to Au. The synthesis of luminescent Ag-Au NCs refers to modified literature reports[1]. Typically, freshly prepared alcoholic solutions of DT (3.6 ml, 50 mM) and AgNO₃ (x ml, 25.4 mM) were mixed well under vigorous stirring for 10 min, the solution was opacified due to the formation of Au(I)-thiolate. Freshly prepared alcoholic solutions of HAuCl₄ (0.2 ml, 25.4 mM) were then added into the mixture solution, the mixture stirred for another 12 h and then incubated overnight at room temperature. The feeding ratio of Ag to Au varied from 0 to 4, in which the volume of HAuCl₄ precursor was constant only change the volume of AgNO₃ solution from 0 ml to 0.8 ml). The samples denoted as Ag_xAu@DT NCs, which the X represented the feeding ratio of Ag to Au. The as synthesized Ag_xAu@DT NCs were used without purification.

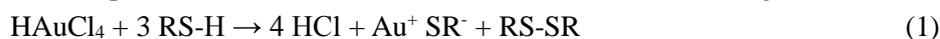
Characterization

Ultraviolet visible (UV-vis) spectroscopy was conducted with a UV2700 UV-vis spectrophotometer. Fluorescence was measured by using a FluorMax-4 fluorimeter (Horiba, Japan). HR-TEM images of NCs were collected with a JEOL JEM 2010 microscope operating at 200 kV. Fluorescence lifetime was measured with a homebuilt time-correlated single photon counting (TCSPC) system with a time resolution of sub-100 ps. Phosphorescence lifetime was excited with a μ F2 lamp and measured with FLS 980 spectrofluorimeter (Edinburgh Instruments). Thermogravimetric analysis (TGA) was conducted on a NETZSCH STA449F3 analyzer under air atmosphere (flow rate of 50 mL min⁻¹). Inductively coupled plasma (ICP) atomic emission spectroscopy was performed on a Thermo IRIS Intrepid II XSP atomic emission spectrometer. X-ray photoelectron spectra (XPS) were measured on an AXIS

SUPRA instrument with X-Ray monochromatisation.

pH Sensing

The stock solution of as-synthesized Ag₁Au@DT NCs was acidic due to the reduction of Au (III) precursors and the formation of thiolate as the following two chemical equations:



The mole amount of H⁺ of the stock solution (4 ml) of as-synthesized Ag₁Au@DT can be estimate about 0.025 mmol according to the equations. To evaluate the sensitivity of pH for as-synthesized Ag₁Au@DT, 0.3 ml stock solution, which contained 1.875 nmol of H⁺, was diluted by adding 1.5 ml ethanol. Different volume of 50 mM NaOH aqueous solution (0 ul, 10 ul, 15 ul, 20 ul, 25 ul, 30 ul, 35 ul, 40 ul and 45 ul corresponding to 0 nmol, 0.5 nmol, 0.75 nmol, 1.0 nmol, 1.25 nmol, 1.5 nmol, 1.75 nmol, 2.0 nmol and 2.25 nmol of OH⁻, respectively). The photoluminescence emission spectra of OH⁻ adjusted Ag₁Au@DT NCs solution after standing overnight were record. The cyclic switching of the pH regulated PL intensity were performed by adding 50 ul 50 mM NaOH and 50 ul 50 mM HCl aqueous solution circularly. The solution of each cycle was ultrasonically treated 5 min before recording the photoluminescence emission spectra.

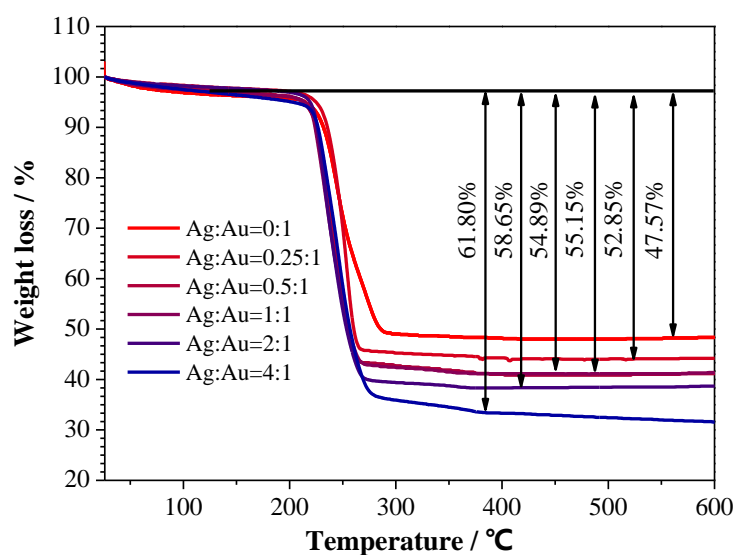


Figure S1. Thermalgravimetric analysis (TGA) of Ag_xAu@DT NCs with different ratio of Ag to Au.

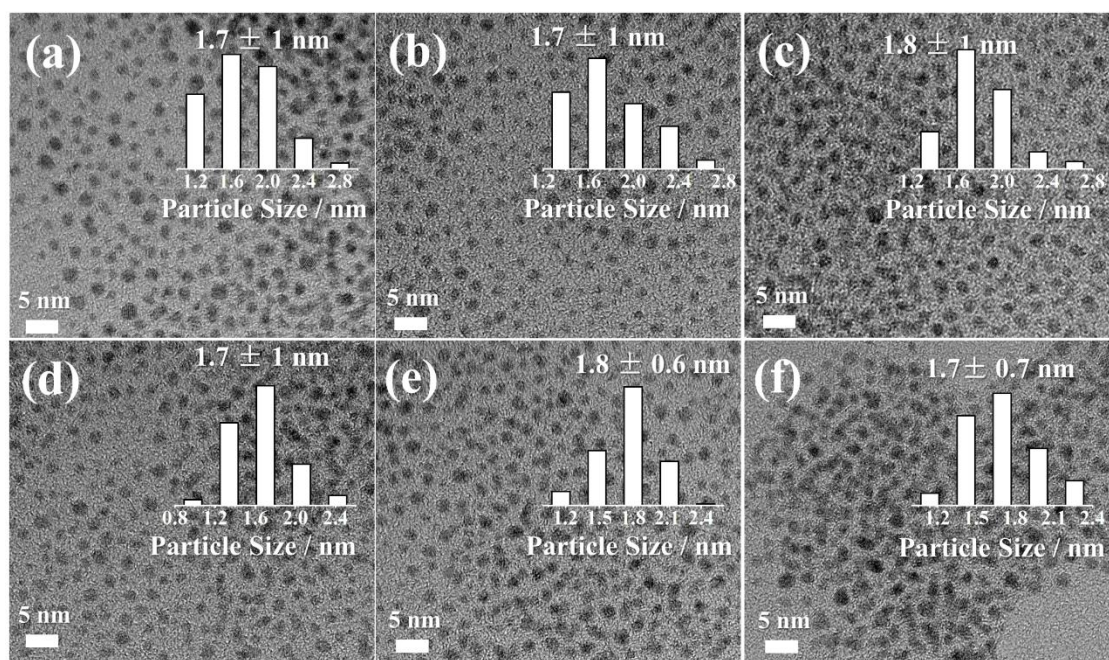


Figure S2. HRTEM micrograph of Ag₀Au@DT (a), Ag_{0.25}Au@DT (b), Ag_{0.5}Au@DT (c), Ag₁Au@DT (d), Ag₂Au@DT NCs (e) and Ag₄Au@DT NCs (f), respectively. The scale bar is 10 nm. The inset shows the size distribution.

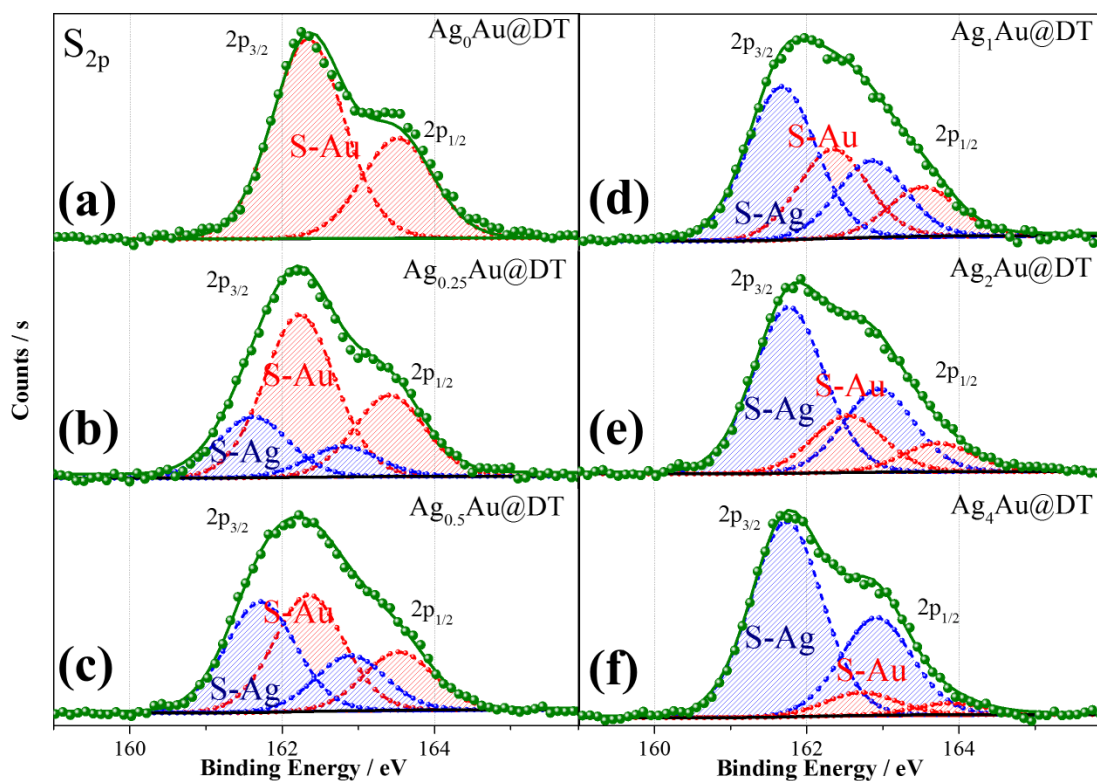


Figure S3. XPS spectrum of S 2p for Ag₀Au@DT (a), Ag_{0.25}Au@DT (b), Ag_{0.5}Au@DT (c), Ag₁Au@DT (d), Ag₂Au@DT NCs (e) and Ag₄Au@DT NCs (f), respectively.

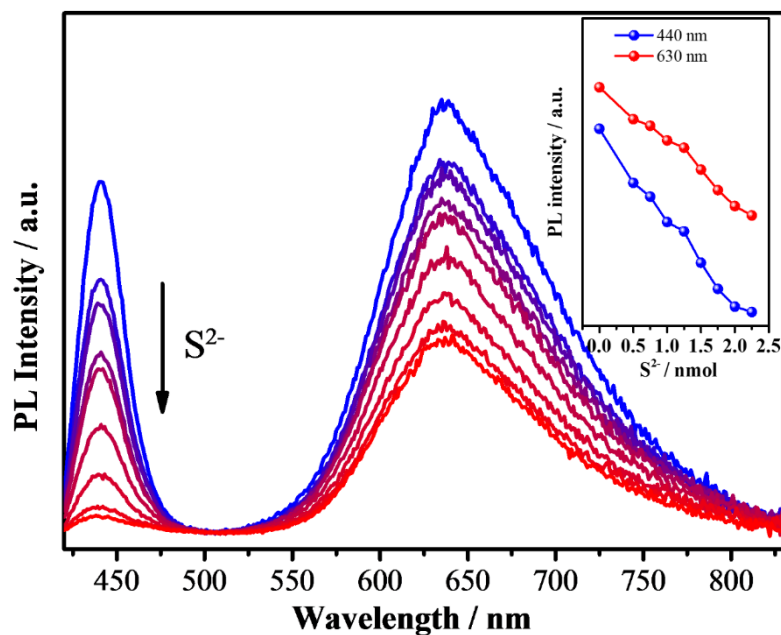


Figure S4. Photoluminescence spectra of as-synthesized $\text{Ag}_1\text{Au@DT}$ NCs after adding increasing amount (0, 0.5, 0.75, 1.0, 1.25, 1.5, 1.75, 2.0 and 2.25 nmol) of 50 mM K_2S aqueous solution. The inset displays the relationship between photoluminescence (440 nm and 630 nm) intensity and the added mole amount of K_2S .

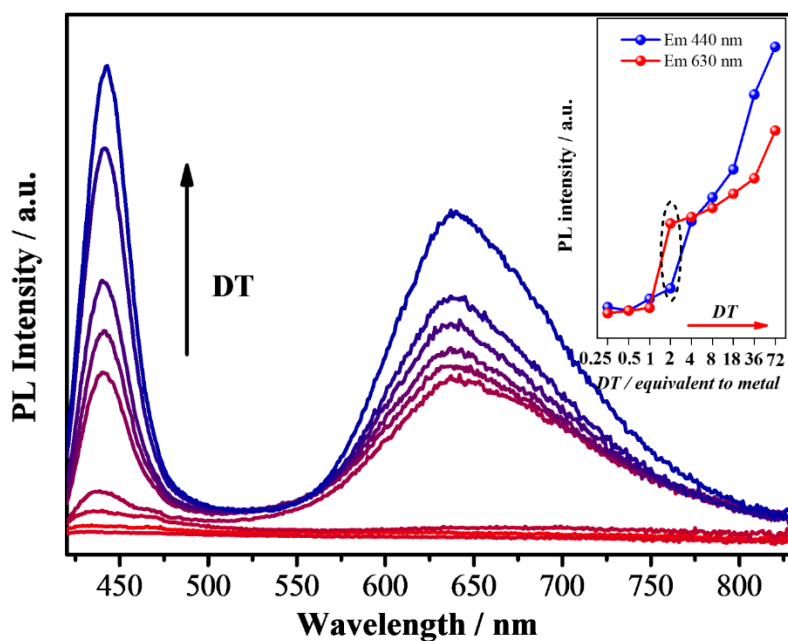


Figure S5. PL emission spectra of $\text{Ag}_1\text{Au@DT}$ NCs synthesized at increasing DT concentration (0.25, 0.5, 1, 2, 4, 8, 18, 36 and 72 equivalent to metal, respectively). The inset displays the relationship between photoluminescence (440 nm and 630 nm) intensity and the amount of DT equivalent to metal.

Table S1. The ratio of Ag to Au of Ag_xAu@DT NCs determined by ICP-OES analysis.

<i>Sample</i>	<i>The molar ratio of Ag-Au</i>		<i>Stoichiometric Formula^a</i>
	<i>Feed</i>	<i>ICP</i>	
<i>Ag₀Au@DT NCs</i>	<i>0</i>	<i>-</i>	<i>Ag₀Au₁DT_{0.9}</i>
<i>Ag_{0.25}Au@DT NCs</i>	<i>0.25</i>	<i>0.11</i>	<i>Ag_{0.1}Au₁DT_{1.2}</i>
<i>Ag_{0.5}Au@DT NCs</i>	<i>0.5</i>	<i>0.23</i>	<i>Ag_{0.2}Au₁DT_{1.4}</i>
<i>Ag₁Au@DT NCs</i>	<i>1</i>	<i>0.47</i>	<i>Ag_{0.5}Au₁DT_{1.5}</i>
<i>Ag₂Au@DT NCs</i>	<i>2</i>	<i>1.02</i>	<i>Ag₁Au₁DT_{2.2}</i>
<i>Ag₄Au@DT NCs</i>	<i>4</i>	<i>1.25</i>	<i>Ag_{1.3}Au₁DT_{2.7}</i>

^aStoichiometric formula was estimated by the calculation of DT to metal weight ratio (TG analysis) and Ag to Au molar ratio (ICP analysis) of Ag_xAu@DT NCs.

Table S2. XPS peak parameters for the S state (Fig. S4) of Ag_xAu@DT NCs.

<i>Sample</i>	<i>Atom</i>	<i>Item</i>	<i>Position (eV)</i>	<i>Content (%)</i>
<i>Ag₀Au@DT NCs</i>	<i>S 2p</i>	<i>Ag(I)-SR</i>	<i>161.6</i>	<i>-</i>
		<i>Au(I)-SR</i>	<i>162.3</i>	<i>100</i>
<i>Ag_{0.25}Au@DT NCs</i>		<i>Ag(I)-SR</i>	<i>161.6</i>	<i>27.3</i>
		<i>Au(I)-SR</i>	<i>162.2</i>	<i>72.7</i>
<i>Ag_{0.5}Au@DT NCs</i>		<i>Ag(I)-SR</i>	<i>161.7</i>	<i>48.7</i>
		<i>Au(I)-SR</i>	<i>162.3</i>	<i>51.3</i>
<i>Ag₁Au@DT NCs</i>		<i>Ag(I)-SR</i>	<i>161.7</i>	<i>63.2</i>
		<i>Au(I)-SR</i>	<i>162.3</i>	<i>36.8</i>
<i>Ag₂Au@DT NCs</i>	<i>Ag(I)-SR</i>	<i>161.8</i>	<i>74.4</i>	
	<i>Au(I)-SR</i>	<i>162.5</i>	<i>25.6</i>	
<i>Ag₄Au@DT NCs</i>	<i>Ag(I)-SR</i>	<i>161.7</i>	<i>88.5</i>	
	<i>Au(I)-SR</i>	<i>162.7</i>	<i>10.5</i>	

Table S3. XPS peak parameters for the O (Fig. 4b) states of Ag_xAu@DT NCs

<i>Sample</i>	<i>Atom</i>	<i>Item</i>	<i>Position (eV)</i>	<i>Content (%)</i>
<i>Ag₀Au@DT NCs</i>		<i>Au⁺-OH</i>	531.8	52.4
		<i>Ag⁺-H₂O</i>	-	-
		<i>Au⁰-H₂O</i>	533.2	47.6
<i>Ag_{0.25}Au@DT NCs</i>	<i>O 1s</i>	<i>Au⁺-OH</i>	531.8	39.7
		<i>Ag⁺-H₂O</i>	532.3	25.0
		<i>Au⁰-H₂O</i>	533.2	35.3
<i>Ag_{0.4}Au@DT NCs</i>		<i>Au⁺-OH</i>	-	-
		<i>Ag⁺-H₂O</i>	532.3	100
		<i>Au⁰-H₂O</i>	-	-

1. Ye, T. and X. An, *Synthesis and properties of Au–Ag bimetallic nanoclusters with dual-wavelength emission*. *New J. Chem.*, 2019. **43**(2): p. 569-572.